Eawag 05234

Comparison of instantaneous and constant-rate stream tracer experiments through non-parametric analysis of residence time distributions

Robert A. Payn,[1] Michael N. Gooseff,[2] David A. Benson,[1] Olaf A. Cirpka,[3] Jay P. Zarnetske,[4] W. Breck Bowden,[5] James P. McNamara,[6] and John H. Bradford[6]

[1] Artificial tracers are frequently employed to characterize solute residence times in stream systems and infer the nature of water retention. When the duration of tracer application is different between experiments, tracer breakthrough curves at downstream locations are difficult to compare directly. We explore methods for deriving stream solute residence time distributions (RTD) from tracer test data, allowing direct, non-parametric comparison of results from experiments of different durations. Paired short- and long-duration field experiments were performed using instantaneous and constant-rate tracer releases, respectively. The experiments were conducted in two study reaches that were morphologically distinct in channel structure and substrate size. Frequency- and time domain deconvolution techniques were used to derive RTDs from the resulting tracer concentrations. Comparisons of results between experiments of different duration demonstrated few differences in hydrologic retention characteristics inferred from short- and long-term tracer tests. Because non-parametric RTD analysis does not presume any shape of the distribution, it is useful for comparisons across tracer experiments with variable inputs and for validations of fundamental transport model assumptions.

1. Introduction

[2] The fate and transport of stream solutes are strongly influenced by the residence time of water in the stream channel and hydrologically connected systems. The overall residence time of water in a stream system is distributed by complex flow paths through the mobile water column, surface pools, lateral dead zones, and substrate pore space, or hyporheic zone [*Hynes*, 1974; *Bencala and Walters*, 1983; *Gooseff et al.*, 2005b]. Solute residence time distributions (RTDs) in stream reaches are commonly characterized through the release of a soluble, conservative tracer into the stream water [*Bencala and Walters*, 1983; *Stream Solute Workshop*, 1990; *Harvey and Wagner*, 2000;

Runkel, 2002]. After the tracer travels a stream length of interest, the downstream concentration is measured over time. The shape of the resulting concentration breakthrough curve (BTC) is determined by the residence time of the dissolved tracer in the stream reach relative to the time it was released. There are two common timescales for tracer releases: (1) In an instantaneous release, a dissolved tracer mass is introduced to the stream over a very short period of time (on the order of seconds). The duration of application is considered instantaneous because it is negligible relative to the time of advective transport through the reach. (2) In a constant-rate release, a solution of known tracer concentration is applied at a steady rate (volume per time) until the downstream concentration reaches a constant value. The "plateau" in downstream tracer concentration resulting from the constant load indicates that the total mass of tracer resident in the reach is at quasi-steady state. This work tests if RTDs derived from the measured BTCs of instantaneous and constant-rate tracer experiments are similar, which would suggest that the effects of tracer storage in the described study stream reaches were linear with concentration and independent of time.

[3] If tracer storage is nonlinear with concentration or dependent on time, RTDs from the described tracer tests may be different due to dramatically different tracer concentration dynamics between constant-rate and instantaneous experiments. In instantaneous release experiments, the stream is subject to a relatively high peak concentration

[1]Hydrologic Science and Engineering Program/Department of Geology and Geological Engineering, Colorado School of Mines, Golden, Colorado, USA.
[2]Department of Civil and Environmental Engineering, Pennsylvania State University, University Park, Pennsylvania, USA.
[3]Swiss Federal Institute of Aquatic Science and Technology (EAWAG), Dübendorf, Switzerland.
[4]Department of Geosciences, Oregon State University, Corvallis, Oregon, USA.
[5]Rubenstein School of the Environment and Natural Resources, University of Vermont, Burlington, Vermont, USA.
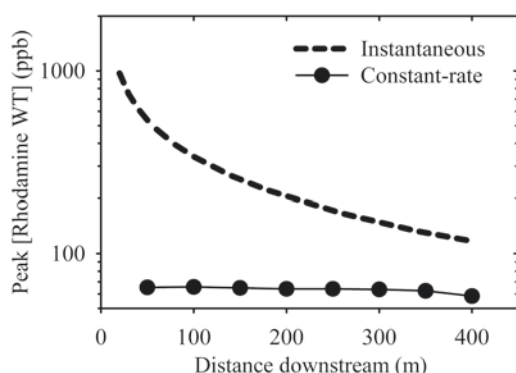[6]Department of Geosciences, Boise State University, Boise, Idaho, USA.

Figure 1. Example peak concentrations of a tracer in a stream reach during instantaneous and constant-rate experiments under similar hydrologic conditions. Instantaneous concentrations were estimated using model parameters from an advection-dispersion-storage transport model fitted to the empirical downstream concentration response to the instantaneous release. Constant-rate concentrations were measured from samples taken at steady state.

over a short duration. Because of the redistribution of tracer mass by dispersive mechanisms, the BTC exhibits decreasing peak concentration and broader distribution with downstream travel distance. In experiments with constant-rate release, by contrast, the peak concentration in the thalweg of the reach is independent of dispersion and is only affected by reach water balance under well-mixed conditions (e.g., dilution from lateral inflow). Therefore in streams without substantial lateral inflow, a constant-rate release results in a relatively consistent peak tracer concentration over the reach (Figure 1). During an instantaneous release experiment, retention mechanisms of the reach, such as dead zones and the hyporheic zone, are exposed to substantially higher tracer concentrations for a shorter, more variable duration in comparison to a constant-rate experiment. With these differences in tracer concentration distribution and exposure times, substantial nonlinearity of tracer retention with concentration or time-scale dependence of tracer retention should be readily evident in comparison of RTDs between the two experiment types.

[4] Any chemical reactivity of the hydrologic tracer is another potential nonlinear influence on observed solute behavior. For example, some studies have reported irreversible sorption of Rhodamine WT [*Smart and Laidlaw*, 1977; *Trudgill*, 1987; *Sabatini and Laidlaw*, 1997; *Lin et al.*, 2003; *Dierberg and DeBusk*, 2005], which is the tracer used in this study. In addition, mass loss of Rhodamine WT has been observed in stream systems [*Bencala et al.*, 1983, 1986]. However, it is not yet clear how the reactivity of Rhodamine WT in the stream environment might affect the RTD. While the RTD comparison of this work is insensitive to any process that is linear with concentration, it will indicate if there is substantial nonlinearity in the fate of the tracer used (i.e., sorption or decay of Rhodamine WT).

[5] The most common approach to analyzing stream hydrologic residence time characteristics is parametric, where a solute transport model is used to simulate the observed BTC [*Runkel*, 1998; *Haggerty et al.*, 2002]. In

effect, this is mathematically identical to describing the stream reach RTD with a particular density function (e.g., inverse Gaussian, exponential, power law, gamma, or combinations thereof). Parameter values are typically determined algorithmically by changing the input parameters until the model output fits the measured BTC [*Bencala and Walters*, 1983; *Stream Solute Workshop*, 1990; *Harvey et al.*, 1996; *Gooseff et al.*, 2005a]. Then, stream hydrologic behavior is compared quantitatively considering the fitted parameters. Recent studies [*Haggerty et al.*, 2002; *Wörman et al.*, 2002] have demonstrated that the most popular quantitative models simulating first-order mass exchange with hydrologic storage (i.e., transient storage [*Bencala and Walters*, 1983]) do not always adequately represent stream RTDs, particularly at late times. Comparison of modeled parameters can therefore mask true differences in stream residence times because they do not adequately describe stream RTDs or the parameters are not sensitive to the parts of RTDs that differ. For constant-rate BTCs, in particular, it might be possible to fit an inadequate parametric distribution to the measured BTC without realizing that important features of the true RTD are missing. Some examples of features not fit by standard transport models are broad peaks or multimodality, which are not generally expected in a stream experiment, but have been observed in groundwater transport studies [*Cirpka et al.*, 2007]. In this work, we refer to the ''shape'' of an RTD as the plot of its PDF, which summarizes the relevant features (e.g., peak height, width, tailing behavior, etc.) necessary for RTD comparison. Although the parametric approach may quantify which specific hydrologic mechanisms (e.g., exchange with transient storage) potentially generate the observed differences in tracer response, it does not necessarily allow detailed description of how the shape described by the RTD random variables might differ. In fact, conclusions about those hydrologic mechanisms may be inaccurate if the parametric model cannot adequately fit the observed BTC.

[6] Previous work has documented parametric differences between instantaneous and constant-rate experimental results from the same stream reach [*Jin and Ward*, 2005], but there is little in existing analyses that suggests why parameter values might vary between tests. In a modeling exercise, *Wagner and Harvey* [1997] demonstrate that transient storage model parameters [*Bencala and Walters*, 1983] are determined with more certainty from a constant-rate experiment than an instantaneous experiment. While this work addresses uncertainty in particular conceptual processes indicated by the model parameters, it does not address the similarity or dissimilarity in the basic information obtained from field tracer tests. In planning tracer experiments, it is important to understand whether the two techniques truly provide different information, not just whether they behave differently in a model fitting algorithm. For a more robust assessment of differences between experiments of different duration, we required direct comparison of the derived stream RTDs without relying on parametric models, that is, without assuming a particular shape of the density function. Therefore we determined RTDs from instantaneous and constant-rate tracer experiments in two morphologically distinct study reaches and investigated whether different conclusions about hydrologic
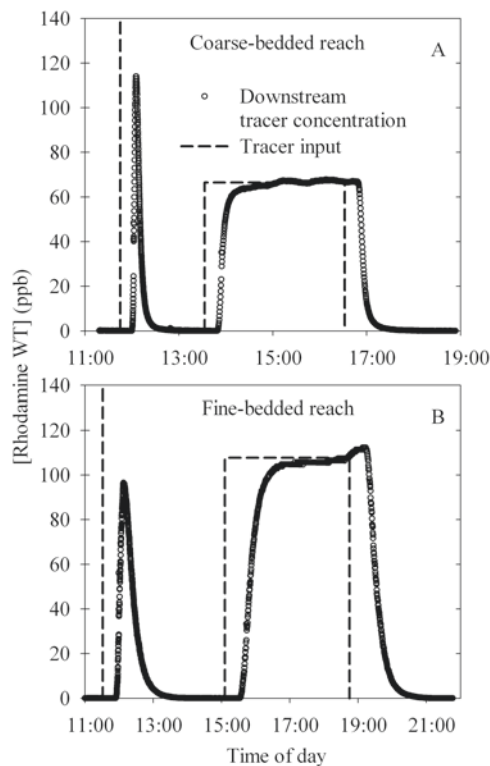
Figure 2. BTCs from (a) the coarse-bedded reach and (b) the fine-bedded reach. Dashed lines represent the instantaneous (vertical) and constant-rate (top-hat) input functions. The input functions for constant-rate tests are adjusted to enforce equal areas under input and output functions.

retention might be drawn from tracer experiments of different timescales.

[7] For direct comparison of tracer tests in this study, we used two methods to deconvolve an RTD from each BTC of constant-rate experiments: a Fourier transform approach and a geostatistical inversion approach. For instantaneous experiments, we derived RTDs from the observed BTCs by simple scaling. We compare the RTDs from paired instantaneous and constant-rate tracer experiments to determine if the observed hydrologic response was independent of the duration of tracer application. We repeat this comparison for two stream reaches with different channel structure and bed material, resulting in presumed differences in RTD shape. Results from the two streams are compared to determine if differences in RTDs from the two tracer techniques are more or less evident in RTDs of fundamentally different shape.

2. Methods

2.1. Study Site

[8] We studied two tundra streams on the north slope of the Brooks Range in Alaska, near the Toolik Field Station (68°38′N, 149°38′W). The substrate of tundra streams consists of variably permeable saturated layers that thaw through the summer and are underlain by relatively impermeable permafrost [*Bradford et al.*, 2005; *Brosten et al.*, 2006]. The two chosen study reaches will be referenced by the dominant size of substrate particles, that is, coarse- or

fine-bedded. The coarse-bedded study reach has substrate dominated by cobbles and gravel. The reach length is 400 m with a slope of 0.97% and has a pool-riffle channel structure. The fine-bedded study reach is in a nearby peat stream. This reach is 250 m long with a slope of 0.90% and consists of a beaded channel structure with wide and deep pools connected by short, deep narrow runs (see *Zarnetske et al.* [2007] for details).

[9] These reaches were chosen due to assumed differences in hydrologic storage characteristics. It was expected that results from the coarse-bedded reach would reflect more hyporheic storage in substrate pore space while results from the fine-bedded reach would reflect more surface storage in the large pools. While this study was not designed to determine the specific mechanisms causing different hydrologic storage, these expectations were the basis of our assumption (verified later) that we were conducting tracer experiments in reaches with fundamentally different RTDs.

2.2. Field Tracer Experiments

[10] On separate days, back-to-back instantaneous and constant-rate tracer experiments were performed in each study reach (Figure 2). Each morning, a known mass of dissolved Rhodamine WT (Bright Dyes, Inc., Miamisburg, OH) was released at the upstream end of one study reach. After the stream channel fluorescence returned to background values, a constant-rate drip of Rhodamine WT was added to the same stream at the same location until the concentrations over the reach were at steady state. During all experiments, Rhodamine WT concentration was measured in situ at the downstream end of each study reach using a Turner 10-AU fluorometer with flow-through cell and data logger (Turner Designs Inc., Sunnyvale, CA). Rhodamine WT concentrations were logged at either 5- or 20-second intervals.

[11] Experiments in the coarse-bedded reach occurred on 18 August 2004. The instantaneous release was 20 g of Rhodamine WT and the constant-rate release was 23 mg/s. In the coarse-bedded reach, discharge calculated by dilution gauging from the instantaneous experimental results was 0.344 m^3/s and discharge calculated from the constant-rate experimental results was 0.343 m^3/s. Experiments in the fine-bedded reach were performed on 16 August 2004. The instantaneous release was 40 g of Rhodamine WT and the constant-rate release was 31 mg/s. In the fine-bedded reach, discharge calculated from the instantaneous experimental results was 0.257 m^3/s and discharge calculated from the constant-rate experimental results was 0.290 m^3/s. While the difference in discharge estimates in the fine-bedded reach was about 12%, it should be noted that tracer mass loss over the reach, either hydrologic or reactive, would result in overestimation of discharge using dilution gauging methods. For all experiments, the target peak downstream concentration of Rhodamine WT was approximately 100 ppb (e.g., Figure 2), above which measurements are incorrect given the calibration of the fluorometer. Achieving the highest concentration measurable was desired to get the most precision in BTC tail measurement. It was later discovered that the Rhodamine WT powder used actually consisted of only about 20% active ingredient. While this knowledge would have allowed higher target concentrations, it does not affect our calculations because
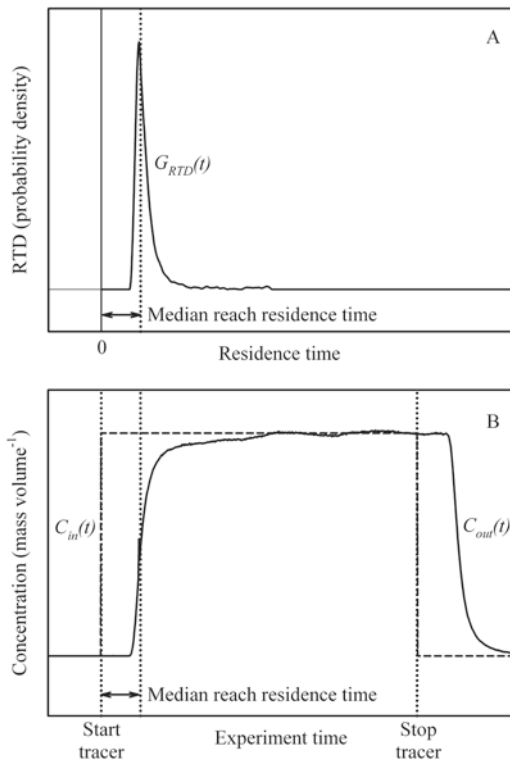
Figure 3. Example of (a) deconvolved RTD and (b) source input (dashed line) and output (solid line) functions for a constant-rate tracer experiment over a stream reach. The input function is adjusted to enforce mass balance, and therefore calculate an RTD of recovered tracer only.

the Rhodamine WT product used to make calibration standards was the same as that used to make release solutions. Therefore all Rhodamine WT masses and concentrations reported are relative to the total mass of product rather than mass of the fluorescent active ingredient.

2.3. Computation of RTDs

2.3.1. Theory

[12] If stream transport and retention of solutes can be described by a linear governing equation with time-invariant coefficients, the tracer BTC measured at the downstream end of a reach ($C_{out}(t)$) is the convolution of the input function ($C_{in}(t)$) and the RTD described by a Green function ($G_{RTD}(t)$):

$$C_{out}(t) = C_{in}(t) * G_{RTD}(t) = \int_0^t C_{in}(\tau) G_{RTD}(t-\tau) d\tau \quad (1)$$

[13] For a stream tracer experiment, $C_{in}(t)$ can either be derived from the tracer application method or be directly measured at the upstream end of the study reach. The Green function describes the system response to a Dirac input function (i.e., a unit impulse). Therefore the Green function derived from any tracer application experiment with a given $C_{in}(t)$ is comparable to a normalized stream reach response to an instantaneous tracer release. Considering only the fraction of tracer mass recovered in the downstream chan-

nel, we scale the input function so that the time integral of $C_{in}(t)$ equals that of $C_{out}(t)$. Therefore the integral of the Green function from our analysis is unity. This Green function may be interpreted as a probability density function (PDF) of residence time (Figure 3a) describing the probability that measured tracer mass spent a particular time in the experimental stream reach.

[14] To force the area under $C_{in}(t)$ to equal the area under $C_{out}(t)$ for constant-rate experiments with a duration of tracer drip t_{drip}, $C_{in}(t)$ was derived as a "top-hat" function (Figure 3b) with a height generating the same total area as observed in $C_{out}(t)$:

$$C_{in}(t) = \begin{cases} \dfrac{\int_0^\infty C_{out}(t) dt}{t_{drip}} & t \in t_{drip} \\ \\ 0 & \text{otherwise} \end{cases} \quad (2)$$

Conceptually, this enforces mass conservation over the reach during the constant-rate experiment release time t_{drip} and produces RTDs of only the recovered tracer. While this is clearly not an appropriate physical assumption, it is outside the scope of this work to compare the mass recovery resulting from the two types of tracer experiments. Therefore for clarity in comparisons, we force RTD results to have an area of unity. If tracer mass recovery is not being considered, then the change in discharge over space (i.e., stream loss and gain) is irrelevant. Finally, we assume that changes in discharge are negligible over experiment time.

[15] For a constant-rate tracer experiment, the unknown is $G_{RTD}(t)$, given the input and output signals $C_{in}(t)$ and $C_{out}(t)$, respectively. We calculated a $G_{RTD}(t)$ from each constant-rate tracer BTC using two numerical deconvolution methods. First, we used the discrete Fourier transform to move $C_{in}(t)$ and $C_{out}(t)$ into the frequency domain, thereby allowing deconvolution by division. Second, we used a time domain smoothing technique developed by *Cirpka et al.* [2007] to overcome amplification of high-frequency "noise" and enforce non-negativity of the determined RTD. Finally, the RTDs from instantaneous tracer experiments were calculated by normalizing the BTC by the mass of tracer applied.

2.3.2. Calculation of RTDs in the Frequency Domain

[16] To transform the discrete time signals $C_{in}(t)$ and $C_{out}(t)$ to the frequency domain, we used the fast Fourier transform algorithm (FFT). The discrete functions were represented by time-dimensioned vectors, which were extended with zero values to avoid computational artifacts caused by the implicit assumption of periodicity underlying the Fourier transform (wrap-around effects). Because the original constant-rate experiment data were sampled at 20-second intervals, the transformed vectors represent the range of component frequencies between 0 and 0.025 s^{-1} (half the sampling frequency). The transformed vectors are the discrete representation of the Fourier transforms of $C_{in}(t)$ and $C_{out}(t)$, denoted $\hat{C}_{in}(f)$ and $\hat{C}_{out}(f)$, respectively. The convolution theorem of the Fourier transform states:

$$\hat{C}_{out}(f) = \hat{C}_{in}(f) \times \hat{G}_{RTD}(f) \; \forall f \quad (3)$$

implying that the Fourier transform $\hat{G}_{RTD}(f)$ of the RTD can be computed by division of $\hat{C}_{out}(f)$ by $\hat{C}_{in}(f)$ at each

frequency. The RTD in the time domain can then be computed by inverse-transformation of $\hat{G}_{RTD}(f)$.

[17] Unfortunately, the inverse-transformed function $G_{RTD}(t)$ from frequency domain division may exhibit physically impossible negative values and unlikely spikes. The exact spectral deconvolution method fails when applied to noisy data because a locally erratic change in $C_{out}(t)$ over just a few sampling intervals can only be described by whole-stream transport process rather than the more likely explanation of experimental error. Because the high-frequency variability is misattributed to tracer residence time, the inverse-transformed $G_{RTD}(t)$ exhibits strong variability at high-frequency. The high frequency variability tends to obscure the physically likely RTD in the results, making them difficult or impossible to interpret. Despite these limitations, we report the frequency domain results from the Fourier transform method to document the problems in applying an obvious deconvolution technique to field data and to illustrate the smoothing effect of the geostatistical inversion method described below.

2.3.3. Calculation of RTDS by Geostatistical Inversion

[18] *Cirpka et al.* [2007] developed a time domain deconvolution technique enforcing smoothness and non-negativity of the determined RTD. In standard geophysical inversion, smoothness is enforced by Tikhonov regularization, in which the squared gradient of the parameter distribution, times a weighting factor, is added to the squared residuals in the objective function [*Tikhonov and Arsenin*, 1977]. In one-dimensional applications, *Kitanidis* [1999] has shown that this regularization is identical to a Bayesian inference scheme assuming a multi-Gaussian prior distribution of the parameter vector with a linear generalized covariance function. The latter implies that the function $G_{RTD}(t)$ is considered a second-order intrinsic random time function with linear semivariogram:

$$\langle G(t) \rangle = \beta \tag{4}$$

$$\langle (G(t) \quad G(t+\tau))^2 \rangle = \gamma(\tau) = \theta|\tau| \tag{5}$$

in which the subscript *RTD* has been dropped for convenience, $\langle \rangle$ denotes the expected value, β is the constant expected value of the prior distribution of $G_{RTD}(t)$ where all values are equally likely, τ is a time increment, $\gamma(\tau)$ is the semivariogram function, and θ is the slope of $\gamma(\tau)$. The semivariogram function $\gamma(\tau)$ quantifies the increasing variability of $G_{RTD}(t)$ with increasing time lag τ. This is analogous to semivariograms in geostatistical descriptions of space-dependent variables.

[19] The slope θ of the semivariogram function $\gamma(\tau)$ is equivalent to the weight of the regularization term in the traditional Tikhonov approach. Putting the inversion into a Bayesian context has the advantage that θ can be rigorously derived from the data by an additional Bayesian inference step. The uncertainty of the determined function $G_{RTD}(t)$ can then be evaluated by generating multiple conditional realizations.

[20] Discretizing the continuous functions $C_{in}(t)$, $C_{out}(t)$, and $G_{RTD}(t)$ using a uniform time increment Δt, leads to the vectors **x**, **y**, and **g** of discrete values, respectively. Then, the convolution integral, equation (1), and the prior statistics of $G_{RTD}(t)$, equations (4) and (5) become:

$$\mathbf{y} = \mathbf{Xg} \tag{6}$$

with $X_{ij} = \Delta t \cdot x_{i-j+1}$

$$\langle \mathbf{g} \rangle = \mathbf{u}\beta \tag{7}$$

$$\langle (\mathbf{g} \quad \mathbf{u}\beta) \otimes (\mathbf{g} \quad \mathbf{u}\beta) \rangle = a\mathbf{u} \otimes \mathbf{u} \quad \mathbf{\Gamma} \tag{8}$$

with $\Gamma_{ij} = \gamma(\Delta t \cdot (i \quad j))$

in which **u** is a vector of unit entries, $\otimes$ denotes a matrix product, a is an arbitrary constant that has no impact on the inference scheme, and $\mathbf{\Gamma}$ is the semivariogram matrix of discrete $G_{RTD}(t)$-values.

[21] The scheme generates multiple conditional realizations of **g** consisting of three contributions: an unconditional realization $\mathbf{g}'_u$ with zero mean and semivariogram matrix $\mathbf{\Gamma}$, a smooth correction term $\mathbf{g}'_c$ with identical prior statistics, and the estimated value of β:

$$\mathbf{g} = \mathbf{g}'_u + \mathbf{g}'_c + \mathbf{u}\beta. \tag{9}$$

The unconditional realization $\mathbf{g}'_u$ is generated by the Cholesky-decomposition technique, whereas $\mathbf{g}'_c$ and β are determined by minimizing the following objective function:

$$W(\mathbf{g}'_c, \beta) = \frac{(\mathbf{y} \quad \mathbf{X}(\mathbf{g}'_u + \mathbf{g}'_c + \mathbf{u}\beta)) \cdot (\mathbf{y} \quad \mathbf{X}(\mathbf{g}'_u + \mathbf{g}'_c + \mathbf{u}\beta))}{\sigma^2}$$
$$\mathbf{g}'^T_c \mathbf{\Gamma}^{-1} \mathbf{g}'_c \tag{10}$$

which penalizes differences between the observed and simulated BTCs in the first term and rapidly varying solutions of $G_{RTD}(t)$ in the second term. The variance σ^2 in the first term expresses experimental error. Non-negativity of **g** is enforced by the method of Lagrange multipliers, which introduces non-linearity into the inference scheme. By including the random vector $\mathbf{g}'_u$, multiple conditional realizations are generated that exhibit the variability expressed by $\gamma(\tau)$ on all scales. The distribution of $G_{RTD}(t)$-values at a given time t is a representation of the uncertainty in estimating the RTD.

[22] The scheme requires two statistical parameters: the variance σ^2 related to experimental error, and the slope θ of the semivariogram. While the first term can easily be determined by enforcing the objective function to meet its expected value, estimating θ is computationally much more demanding. We estimate θ by the expectation-maximization method, which is based on iterative updating of θ after analyzing an entire ensemble of conditional realizations. We refer to *Cirpka et al.* [2007] for further details on the estimation method, as well as the full description of deconvolution by geostatistical inversion.

[23] The outcome of the approach is a set of possible RTDs that predict the measured data within prescribed error bounds and exhibit the fluctuations expressed by the semivariogram function $\gamma(\tau)$. As stated above, choosing a linear semivariogram implies minimizing gradients of $G_{RTD}(t)$ [*Kitanidis*, 1999]. Other models, such as an exponential semivariogram, may require additional parameters (e.g., the range in the case of an exponential model), which are difficult to infer from the data. In fact, large-scale features of the
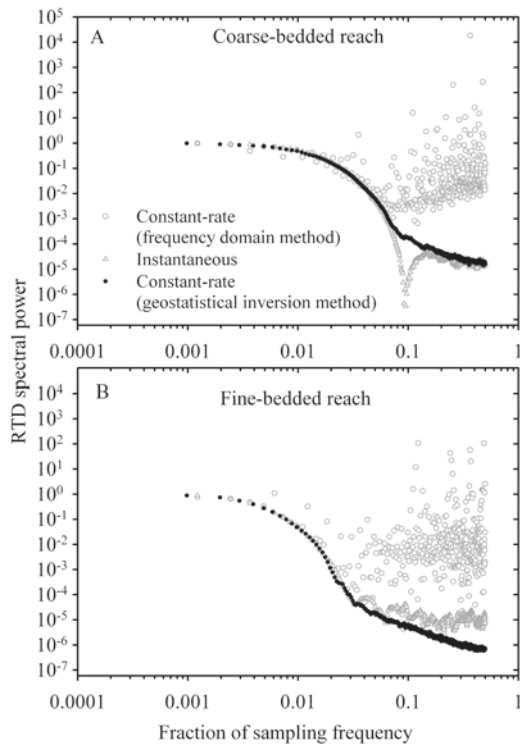
Figure 4. Power spectra of the RTDs derived from constant-rate and instantaneous tracer experiments in (a) the coarse-bedded reach and (b) the fine-bedded reach.

determined RTD are almost completely imposed by the data, so that a semivariogram differing from the linear model only at larger time lags (τ) leads to practically identical estimates of $G_{RTD}(t)$. From the set of RTD realizations, the conditional mean of $G_{RTD}(t)$ can be computed by arithmetic averaging. We report averages of 100 realizations for this work. For comparison in the frequency domain, the discrete Fourier transform was calculated for all 100 realizations and we report the average spectral powers for each frequency.

[24] In summary, the geostatistical inversion technique produces a discrete RTD description with no prior assumption of the distribution shape, except the optimal smoothness indicated by the linear semivariogram and enforced non-negativity. The statistical parameters described above mainly characterize the higher-frequency component of the RTD, which is subject to uncertainty. The lower-frequency signal is well imposed by the experimental data and is much less uncertain. Figure 3 provides examples of the input, output, and deconvolved RTD functions from a constant-rate experiment from this research.

2.3.4. Calculation of RTDs From Instantaneous Release Experiments

[25] Because instantaneous release experiments simulate a Dirac impulse input signal, the RTD of recovered tracer is the downstream BTC normalized to the total area under the BTC curve:

$$G_{RTD}(t) = \frac{C_{out}(t)}{\int\limits_0^\infty C_{out}(\tau)d\tau} \qquad (11)$$

in which we have implied that the tracer was released at time zero. We applied trapezoidal approximation over

sample intervals to numerically integrate the BTC. Using the discrete measured values of the BTC for $C_{out}(t)$, we obtained a vector representing $G_{RTD}(t)$ in the time domain, which was compared to values obtained from the constant-rate experiments. The discrete Fourier transform of the $G_{RTD}(t)$ vector was used for comparisons in the frequency domain.

3. Results

[26] Figure 4 shows power spectra of the RTDs determined from constant-rate experiments and instantaneous experiments. RTDs from constant-rate experiments are presented from both calculation methods: division in the frequency domain and geostatistical inversion in the time domain. The spectra are similar at low frequencies. However, at high frequencies, the spectral power of the constant-rate experiment RTDs determined in the frequency domain is considerably higher and more variable than results from either of the other combinations of experimental and analytical methods. As mentioned above, the high-frequency noise in the RTDs determined by division in the frequency domain leads to strongly fluctuating distributions in the time domain with physically impossible negative values.

[27] For RTDs calculated by geostatistical inversion of constant-rate experiment BTCs, we have assumed that the RTD follows a linear variogram. Through the described inverse modeling, the experimental error, σ, was found to be 0.37 and 0.98 ppb for the coarse- and fine-bedded reaches, respectively. The slope of the variogram, θ, was estimated to be 5.3×10^{-6} and 6.5×10^{-8} min^{-3} for the coarse- and
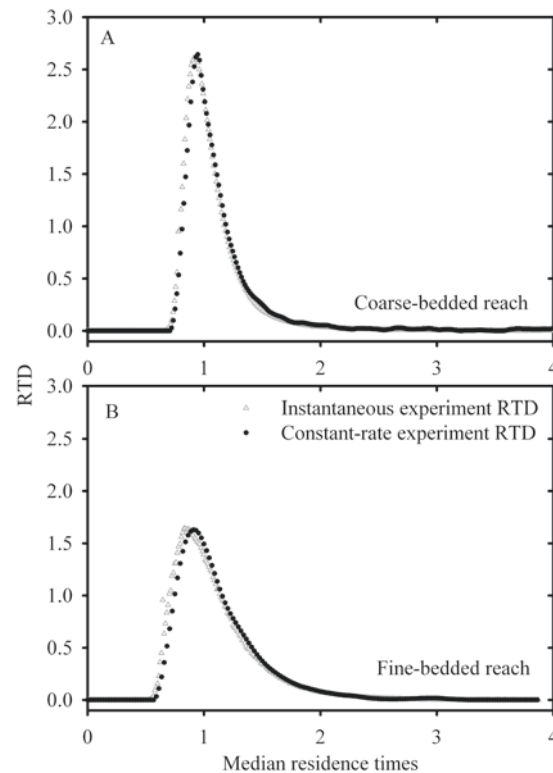

Figure 5. Constant-rate and instantaneous experiment RTDs in the linear domain for (a) the coarse-bedded reach and (b) the fine-bedded reach.
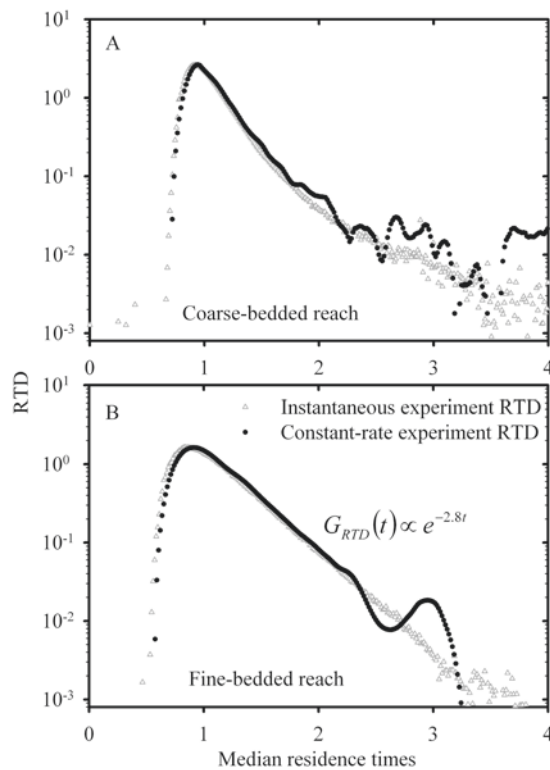
Figure 6. Constant-rate and instantaneous experiment RTDs in the semi-logarithmic domain for (a) the coarse-bedded reach and (b) the fine-bedded reach. An approximate rate of RTD decay for the fine-bedded reach was calculated using regression of the instantaneous experiment RTD probability distribution above 1.1 median residence times. Gaps are zero values that cannot be plotted on a logarithmic scale.

fine-bedded reaches, respectively. The linear variogram model leads, at least in the unconditional contribution $G_u'(t)$, to a power spectrum scaling with θ/f^2, in which f is the frequency. Deviations from this scaling behavior are enforced by conditioning to the data. In the approach of *Cirpka et al.* [2007], the optimal value of θ is determined from the data. However, the linear shape of the variogram causes the high-frequency scaling of the power spectrum with f^{-2} to be fixed. That is, it is difficult to extract the correct spectral power of the RTD when the measured BTCs used in the deconvolution are noisy, particularly for the highest frequencies. It should be noted that the spectra of the RTD shown in Figure 4, as determined by geostatistical inversion, are for the conditional realizations. The conditional mean, that is, the arithmetic mean of all 100 realizations, is smoother resulting in stronger attenuation of high-frequency components.

[28] The RTDs from constant-rate and instantaneous experiments are plotted in linear (Figure 5), semi-logarithmic (Figure 6), and double-logarithmic (Figure 7) space. Time domain RTDs from constant-rate experiments are only shown from the geostatistical inversion technique due to the previously described high frequency noise interference in the Fourier transform method. In these plots, the residence time in each reach was normalized by the median of the distribution (i.e., median transport time), and probability densities were refactored in the normalized timescale. These calculations ensure that the areas under the RTD-curves in Figure 5 are unity, and allows the comparison of the RTD shape between the two stream reaches. The median residence times were calculated numerically from the instantaneous-release RTDs, resulting in values of 22 min for the coarse-bedded reach and 44 min for the fine-bedded reach. For both study reaches, the RTD tails were similar between instantaneous and constant-rate responses. The initial arrivals of tracer were slightly different between the two experimental and analytic methods, where the instantaneous release appears to arrive somewhat earlier than the constant-rate release.

[29] The plots of RTDs on different scales reveal the nature of tracer retention (tailing) and suggest a potential mathematical description of hydrologic storage in the stream reaches. For the coarse-bedded stream, the RTD tail exhibits power law behavior (i.e., $G_{RTD}(t) \propto t^{-4.8}$, Figure 7a). For the fine-bedded stream, RTD tailing exhibits exponential decay (i.e., $G_{RTD}(t) \propto e^{-2.8t}$, Figure 6b).

4. Discussion

[30] The observed similarity in power spectra of the frequency domain RTDs suggest that similar information about hydrologic retention was acquired from instantaneous and
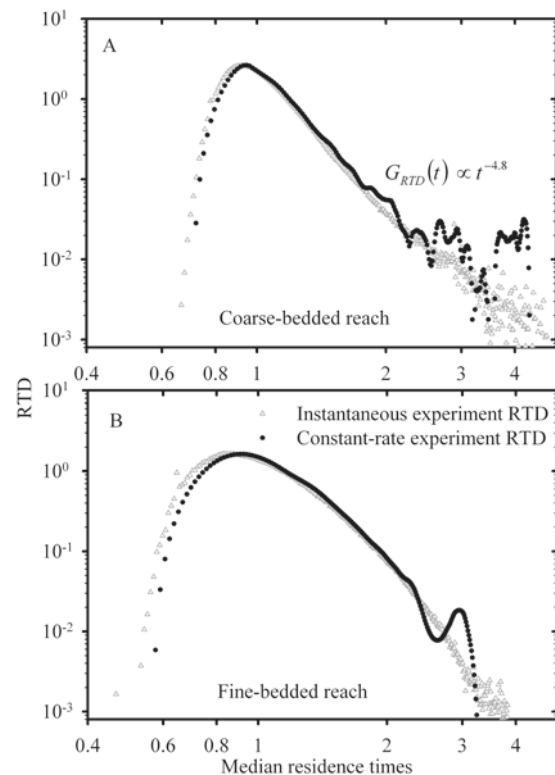

Figure 7. Constant-rate and instantaneous experiment RTDs in the double-logarithmic domain for (a) the coarse-bedded reach and (b) the fine-bedded reach. An approximate rate of RTD decay for the coarse-bedded reach was calculated using regression of the instantaneous experiment RTD probability distribution between 1.8 and 3.6 median residence times. Gaps are zero values that cannot be plotted on a logarithmic scale.

and constant-rate experiments (Figure 4). As discussed above, the spectrum determined by dividing the Fourier transforms of C_{out} and C_{in} differs at high frequencies from the spectra determined from either of the other methods. Back-transformation into the time domain would result in meaningless, strongly fluctuating RTDs, prohibiting the use of direct frequency domain deconvolution of inevitably noisy field data.

[31] The geostatistical inversion technique of *Cirpka et al.* [2007] provides a method to eliminate noise and produce RTDs with variability only at the timescales interesting to whole-stream behavior, specifically those frequencies that compose the RTD. Because time domain RTDs were obtainable in PDF form for both tracer methods, they could be compared directly. This comparison in the time domain allows not only general conclusions about the similarity of the tracer results but also shows the specific times when RTDs may differ.

[32] The RTDs from instantaneous and constant-rate tracer experiments exhibit few differences in shape (Figures 5, 6 and 7). Therefore in these stream reaches, the mechanisms important to solute transport and storage are likely independent of solute concentration during the experiment. This independence suggests a linear model of transport and storage is appropriate. Considering our use of Rhodamine WT, which is measurable at very low concentrations, it is unlikely that other, less detectable tracers would have yielded different results because it is unlikely that other tracers would have more resolution in the tail. Similarity in RTDs also suggests that potential non-conservative behavior of Rhodamine WT [*Bencala et al.*, 1983, 1986; *Sabatini and Austin*, 1991] did not cause differences between instantaneous and constant-rate experimental results. If non-conservative behavior of RWT was measurable in these streams, it must have been nearly linear with tracer concentration, thereby generating equal influence on the RTD of both instantaneous and constant-rate experiments. It is important to note that these conclusions apply only to the RTD of recovered tracer. The overall mass balance of tracer in the reach, as determined by either hydrologic or chemical processes, is not addressed by this approach. Questions regarding the mass balance of contrasting tracer experiments with a potentially non-conservative tracer are left to future work designed specifically for mass flux measurement.

[33] On the surface, the results of this work may seem contradictory to the model uncertainty analysis of *Wagner and Harvey* [1997], where the authors demonstrate that there is more certainty in model parameters derived from constant-rate experiments. However, due to the differences between parametric versus non-parametric analyses, the studies are not directly comparable. In short, our study determines if instantaneous and constant-rate experiments produce similar solute residence time information. By contrast, the Wagner and Harvey study determines which experiment produces information that allows the most certainty in inferring particular hydrologic retention mechanisms. Because our analysis does not rely on any conceptual physical model of hydrologic retention, we find little difference between the information gained from the two experiments. As shown by Wagner and Harvey, however, the similarity in RTDs does not necessarily mean that the

two types of tracer test are equivalent for testing physical transport models, which are capable of simulating and inferring more hydrologic information than just residence time.

[34] Both stream hydraulics and methodology may explain why first arrival of the tracer appears to have been earlier in instantaneous release experiments relative to constant-rate release experiments. A physical explanation may be slightly differing velocities between the experiment times, but this does not reconcile with the discharges measured by dilution gauging. Note, however, that accuracy of dilution gauging depends on the mass balance of tracer during the experiment. Methodological explanations may arise from the best fit algorithms employed by the geostatistical deconvolution technique. Regardless of the source of the discrepancy in first-arrival, it is generally small and unlikely to change conclusions about hydrologic storage based on the presented data. The discrepancy might, however, modestly change the quantification of dispersion based on the RTD.

[35] The tail of the RTD is important for appropriate interpretation of stream solute processing rates. The shape of the tail describes the volume and duration of water retention in the stream system storage zones. In particular, long residence times are typical in stream subsystems with high sediment and microbiological contact [*Triska et al.*, 1989]. Results from recent tracer tests indicate that streams demonstrate fundamentally different hydrologic storage characteristics [*Haggerty et al.*, 2002; *Wörman et al.*, 2002], where the effects of hydrologic storage are most evident in the tail of the observed tracer BTC. Our results reinforce this conclusion in that the fine-bedded stream reflects exponential RTD tailing and the coarse-bedded stream reflects power law tailing. The differences in RTD shape are likely indicators of stream channel structural effects on mechanisms of hydrologic retention. In this case, the differences we observed were probably due to the relative influence of surface versus subsurface storage in the fine- and coarse-bedded study reaches. For more information in this area, *Zarnetske et al.* [2007] have compared hydrologic storage data among a larger and more diverse set of stream reaches in the study area. Further research is needed to directly distinguish between surface and subsurface hydrologic retention in stream tracer RTDs, a distinction necessary for more mechanistic models of reactive solute fate and transport.

[36] The results of the geostatistical inversion technique exhibit some limitations in characterizing long-term residence times. In the RTD data above 2 median residence times, the imprecision of the constant-rate RTD relative to the instantaneous RTD is evident in results from both reaches (Figure 6). Most of these errors likely stem from imprecision in the BTC toward the end of the plateau phase during the constant-rate experiments (e.g., Figure 3a). Analytically, measurement of small changes in concentration is less reliable at high concentrations than at low concentrations. Therefore small changes in the BTC near plateau in the middle of the constant-rate experiment are more difficult to measure than small changes near background fluorescence at the end of the experiment. If the end of the constant-rate experiment is treated as an inverted Heaviside input function (unit step function), the RTD can be calculated by numerical differentiation of the BTC from

the time the constant-rate release stops to the return to background conditions. In this way, numerical differentiation would consider only the RTD tail evident near background concentrations at the end of the experiment and would therefore be less vulnerable to inherent imprecision in BTCs. However, numerical differentiation of discrete data is subject to similar noise amplification as numerical deconvolution and would require similar smoothing or filtering algorithms. Finally, numerical differentiation is limited to only constant-rate input functions, whereas the technique of *Cirpka et al.* [2007] is applicable to any input function including those directly measured upstream. For these streams, an experiment with instantaneous tracer release provides a similar RTD and more precision at late-time than the given constant-rate experimental analysis.

[37] The differences in RTD shape between the two streams of different structure demonstrate two potential shortcomings of parametric comparisons without initial non-parametric comparison. First, if both of these streams were fit by an exponential tailing model, which is quite common in stream tracer analyses, the power law information in the original BTC would not have been considered. This loss of information would be critical in analysis of variability in fundamental RTD shape across other reaches in the study area [*Zarnetske et al.*, 2007]. Second, while differences in model parameters do suggest the general timing of BTC differences [*Stream Solute Workshop*, 1990], they do not allow the direct comparison of how these differences are reflected in the shape of the RTD. The combined consequence of these two shortcomings is that perceived differences in parameters might be caused either by variability in particular storage mechanisms of a particular conceptual model (e.g., high versus low transient storage) or by fundamental differences in the most appropriate conceptual model (e.g., exponential versus power law tailing). This uncertainty in the cause of parameter differences can be effectively explored through non-parametric comparison.

[38] Many stream system analyses simplify hydrologic effects using a single "average" velocity to quantify solute movement through the system. This simplification is often appropriate when generalizing "black-box" stream reach behavior that includes both hydrologic and biogeochemical function. However, it is becoming clear that consideration of the full velocity distribution is important to understanding particular stream processes. For example, accounting for the entire velocity distribution is important for properly removing the effects of hydrologic transport from measurements of stream biological activity [*Runkel*, 2007]. Initial non-parametric RTD analysis reduces the chances of introducing undue bias from an arbitrary choice of transport model and provides objective support for determining the most appropriate model of velocity distribution for process-based analysis. Finally, an active tracer RTD, which may have a mass less than unity, could be compared to a conservative tracer RTD to identify the residence times of particular importance to biogeochemical processing of the active tracer.

5. Conclusions

[39] Non-parametric characterization of residence-time distributions from tracer experiments with variable inputs is a useful tool for hydrologic analysis. These techniques have been demonstrated with natural fluctuations in solute concentrations at watershed scales [*Kirchner et al.*, 2000] and river bank infiltration into groundwater [*Cirpka et al.*, 2007]. We introduce a similar approach with artificial tracers in streams, demonstrating the utility of RTD deconvolution in reliably estimating the distribution of residence or transport times of a stream reach. From this exercise, we have come to the following conclusions.

[40] (1) The geostatistical inversion technique of *Cirpka et al.* [2007] is efficient in deconvolving stream-reach RTDs from experimental tracer BTCs. Furthermore, the method effectively compensates for the inherent experimental error in BTCs that produce non-interpretable RTDs using traditional frequency domain deconvolution techniques. The geostatistical deconvolution approach is a useful step toward direct, non-parametric comparisons of tracer tests with varying application techniques.

[41] (2) In our study reaches, hydrologic retention characteristics indicated by the RTDs were similar between instantaneous and constant-rate tracer experiments. This similarity was evident in stream RTDs with both exponential and power law tailing, and indicates linear transport models would be appropriate in both cases.

[42] (3) Differences in RTD tailing support previous findings of variability in hydrologic retention behavior. In our case, fundamental differences in RTD shape are most likely due to differences in channel structure and substrate hydraulic conductivity.

[43] (4) In streams similar to our study reaches, instantaneous experiments are likely to provide an RTD similar to constant-rate tests. However, instantaneous RTDs normalized by recovered mass are likely to exhibit more precision in long-term residence times relative to the provided deconvolution analysis of constant-rate data. If only constant-rate data are available and precision in late-time RTD response is desired, we suggest an analysis that minimizes influence of long-term residence data in the plateau and maximizes influence of long-term residence data near background concentrations.

References

Bencala, K. E., and R. A. Walters (1983), Simulation of solute transport in a mountain pool-and-riffle stream: A transient storage model, *Water Resour. Res.*, *19*(3), 718 724.

Bencala, K. E., R. E. Rathbun, A. P. Jackman, V. C. Kennedy, G. W. Zellweger, and R. J. Avanzino (1983), Rhodamine WT dye losses in a mountain stream environment, *Water Resour. Bull.*, *19*(6), 943 950.

Bencala, K. E., D. M. McKnight, G. W. Zellweger, and J. Goad (1986), The stability of rhodamine WT dye in trial studies of solute transport in an acidic and metal-rich stream, in *Water Supply Paper, Tech. Rep. 2310*, pp. 87 95, U.S. Geol. Surv., Colorado.

Bradford, J. H., J. P. McNamara, W. B. Bowden, and M. N. Gooseff (2005), Measuring thaw depth beneath peat-lined arctic streams using ground-penetrating radar, *Hydrol. Processes*, *19*, 2689 2699.

Brosten, T., J. H. Bradford, J. P. McNamara, J. P. Zarnetske, M. N. Gooseff, and W. B. Bowden (2006), Profiles of temporal thaw depths beneath two arctic stream types using ground-penetrating radar, *Permafrost Periglac.*, *17*(4), 341 355.

Cirpka, O. A., M. N. Fienen, M. Hofer, E. Hoehn, A. Tessarini, R. Kipfer, and P. K. Kitanidis (2007), Analyzing bank filtration by deconvoluting time series of electric conductivity, *Ground Water*, *45*(3), 318 328.

Dierberg, F. E., and T. A. DeBusk (2005), An evaluation of two tracers in surface-flow wetlands: Rhodamine-WT and lithium, *Wetlands*, *25*(1), 8 25.

Gooseff, M. N., K. E. Bencala, D. T. Scott, R. L. Runkel, and D. M. McKnight (2005a), Sensitivity analysis of conservative and reactive stream transient storage models applied to field data from multiple-reach experiments, *Adv. Water Resour.*, *28*, 479 492.

Gooseff, M. N., J. LaNier, R. Haggerty, and K. Kokkeler (2005b), Determining in-channel (dead zone) transient storage by comparing solute transport in a bedrock channel - alluvial channel sequence, *Water Resour. Res.*, *41*, W06014, doi:10.1029/2004WR003513.

Haggerty, R., S. M. Wondzell, and M. A. Johnson (2002), Power-law residence time distribution in the hyporheic zone of a 2nd-order mountain stream, *Geophys. Res. Lett.*, *29*(13), 1640, doi:10.1029/2002GL014743.

Harvey, J., and B. Wagner (2000), Quantifying hydrologic interactions between streams and their subsurface hyporheic zones, in *Streams and Groundwaters*, edited by J. B. Jones and P. Mulholland, pp. 3 44, Academic Press, San Diego.

Harvey, J. W., B. J. Wagner, and K. E. Bencala (1996), Evaluating the reliability of the stream tracer approach to characterize stream-subsurface exchange, *Water Resour. Res.*, *32*(8), 2441 2451.

Hynes, H. B. N. (1974), Further studies on the distribution of stream animals within the substratum, *Limnol. Oceanogr.*, *19*, 92 99.

Jin, H., and G. M. Ward (2005), Hydraulic characteristics of a small coastal plain stream of the southeastern United States: Effects of hydrology and season, *Hydrol. Processes*, *19*, 4147 4160.

Kirchner, J. W., X. Feng, and C. Neal (2000), Fractal stream chemistry and its implications for contaminant transport in catchments, *Nature*, *403*, 524 527.

Kitanidis, P. K. (1999), Generalized covariance functions associated with the Laplace equation and their use in interpolation and inverse problems, *Water Resour. Res.*, *35*(5), 1361 1368.

Lin, A. Y., J. Debroux, J. A. Cunningham, and M. Reinhard (2003), Comparison of rhodamine WT and bromide in the determination of hydraulic characteristics of constructed wetlands, *Ecol. Eng.*, *20*, 75 88.

Runkel, R. L. (1998), One dimensional transport with inflow and storage (OTIS): A solute transport model for streams and rivers, in *Water-Resources Investigations*, *Tech. Rep.* 98-4018, US Geol. Surv., Denver, Colo.

Runkel, R. L. (2002), A new metric for determining the importance of transient storage, *J. N. Am. Benthol. Soc.*, *21*(4), 529 543.

Runkel, R. L. (2007), Toward a transport-based analysis of nutrient spiraling and uptake in streams, *Limnol. Oceanogr. Methods*, *5*, 50 62.

Sabatini, D. A., and T. A. Austin (1991), Characteristics of rhodamine WT and fluorescein as ground-water tracers, *Ground Water*, *29*(3), 341 349.

Smart, P. L., and I. M. S. Laidlaw (1977), An evaluation of some fluorescent dyes for water tracing, *Water Resour. Res.*, *13*(1), 15 33.

Stream Solute Workshop (1990), Concepts and methods for assessing solute dynamics in stream ecosystems, *J. N. Am. Benthol. Soc.*, *9*(2), 95 119.

Tikhonov, A. N., and V. Arsenin (1977), *Solution of Ill-Posed Problems*, Winston and Sons, Wash.

Triska, F. J., V. C. Kennedy, R. J. Avanzino, G. W. Zellweger, and K. E. Bencala (1989), Retention and transport of nutrients in a third-order stream in northwestern California: Hyporheic processes, *Ecology*, *70*(6), 1893 1905.

Trudgill, S. T. (1987), Soil water dye tracing, with special reference to the use of rhodamine WT, lissamine FF, and amino G acid, *Hydrol. Processes*, *1*, 149 179.

Wagner, B. J., and J. W. Harvey (1997), Experimental design for estimating parameters of rate-limited mass transfer: Analysis of stream tracer studies, *Water Resour. Res.*, *33*(7), 1731 1741.

Wörman, A., A. I. Packman, H. Johansson, and K. Jonsson (2002), Effect of flow-induced exchange in hyporheic zones on longitudinal transport of solutes in streams and rivers, *Water Resour. Res.*, *38*(1), 1001, doi:10.1029/2001WR000769.

Zarnetske, J. P., M. N. Gooseff, T. R. Brosten, J. H. Bradford, J. P. McNamara, and W. B. Bowden (2007), Transient storage as a function of geomorphology, discharge, and permafrost active layer conditions in arctic tundra streams, *Water Resour. Res.*, *43*, W07410, doi:10.1029/2005WR004816.

————————————

D. A. Benson and R. A. Payn, Hydrologic Science and Engineering Program/Department of Geology and Geological Engineering, Colorado School of Mines, 1516 Illinois St., Golden, CO 80401, USA. (rpayn@mines.edu)

W. B. Bowden, Rubenstein School of the Environment and Natural Resources, University of Vermont, 304 Aiken Center, Burlington, VT 05405, USA.

J. H. Bradford and J. P. McNamara, Department of Geosciences, Boise State University, MS-1535, 1910 University Drive, Boise, ID 83725-1535, USA.

O. A. Cirpka, Swiss Federal Institute of Aquatic Science and Technology (EAWAG), Überlandstrasse 133, P.O. Box 611, 8600, Dübendorf, Switzerland.

M. N. Gooseff, Department of Civil and Environmental Engineering, Pennsylvania State University, University Park, PA 16802, USA.

J. P. Zarnetske, Department of Geosciences, Oregon State University, 104 Wilkinson Hall, Corvallis, OR 97331, USA.